Energy 239 (2022) 122152

Contents lists available at ScienceDirect

Energy

journal homepage: www.elsevier.com/locate/energy

Weather-induced variability of country-scale space heating demand under different refurbishment scenarios for residential buildings

Francesco Lombardi [a, d, *], Matteo Vincenzo Rocco [a], Lorenzo Belussi [b], Ludovico Danza [b], Chiara Magni [c], Emanuela Colombo [a]

[a] Politecnico di Milano, Department of Energy, Milan, Italy
[b] National Research Council of Italy, Construction Technologies Institute (ITC-CNR), San Giuliano Milanese, Italy
[c] KU Leuven, Faculty of Engineering Technology, Geel, Belgium
[d] TU Delft, Department of Engineering Systems and Services, Delft, Netherlands

ARTICLE INFO

Article history:
Received 19 January 2021
Received in revised form
12 August 2021
Accepted 22 September 2021
Available online 24 September 2021

Keywords:
Heat demand simulation
Weather regimes
Nearly zero energy buildings
Lumped-parameter approach
Energy modelling

ABSTRACT

The decarbonisation of residential heat through integration with the power system and deployment of refurbishment policies is at the core of European energy policies. Yet, heat-electricity integration may be challenged, in practice, by the large variability of heat demand across weather years. Current approaches for residential heat demand simulation fail to provide insights about the extent of such variability across many weather years and about the benefits potentially brought about by nearly zero-energy buildings. To fill this gap, this work develops an open-source space-heating demand simulation workflow that is applicable to any country's building stock. The workflow, based on a well-established lumped-parameter thermodynamic model, allows capturing sub-national weather-year variability and the mitigation effects of refurbishment. For Italy, different weather years lead to variations in heat demand up to 2 TWh/day, lasting for several days. Moreover, some weather regimes produce spatial asymmetries that may further complicate heat-electricity integration. The refurbishment of about 55% of buildings constructed before 1975 could substantially mitigate such oscillations, leading to a 31–37% reduction of yearly heat demand, primarily in colder regions. Intra-day heat demand variations, driven by user behaviour, are not substantially impacted by refurbishment, calling for the simultaneous deployment of flexible heat generating technologies.
© 2021 The Author(s). Published by Elsevier Ltd. This is an open access article under the CC BY license (http://creativecommons.org/licenses/by/4.0/).

1. Introduction

The achievement of internationally-agreed climate mitigation targets requires a rapid and deep decarbonisation of all energy end uses [1]. In the European Union (EU), aiming to be carbon-neutral by 2050, up to 25% of the total final energy consumption is associated with end uses in residential buildings, with space heating loads largely dominating, with a share of about 64.1%, over water heating (14.8%), electricity for lighting and appliances (14.4%), cooking (5.6%) and cooling (0.3%) [2]. As such, the residential heat sector is at the core of EU decarbonisation long-term plans, aiming at increasing the rate of refurbishment of existing buildings in the direction of nearly zero-energy buildings (NZEBs) [3], and at achieving deeper penetrations of highly-efficient and flexible power-to-heat (P2H) technologies [4]. The foreseen increasing interconnection of power production and residential space-heating supply via P2H, however, raises some challenges. Power systems are already in need of coping with the site-specific and weather-related performances of increasing shares of variable renewable energy sources [5]. The electrification of residential space-heating demand would represent an additional, large source of weather-induced variability that might challenge systems' adequacy – particularly for those countries, such as Italy, that exhibit marked differences of weather regimes across their sub-national entities and bottlenecks in the transmission of electricity between those. To allow a conjoint study of heat demand and renewable generation patterns and support a frictionless coupling of power generation and residential space-heating supply, it is thus critical to provide quantitative insights around the following unanswered research questions:

* Corresponding author. Politecnico di Milano, Department of Energy, Milan, Italy.
E-mail address: f.lombardi@tudelft.nl (F. Lombardi).

https://doi.org/10.1016/j.energy.2021.122152
0360-5442/© 2021 The Author(s). Published by Elsevier Ltd. This is an open access article under the CC BY license (http://creativecommons.org/licenses/by/4.0/).

1. To what extent and at what temporal scale (e.g., hours, days) can residential space-heating demand vary across weather years, at a country scale?
2. To what extend would a realistic penetration of NZEBs alleviate such variability and the overall burden entailed by the electrification of residential space-heating demand?
3. Are there any asymmetries in the variability of heat demand at the sub-national scale – such as regions experiencing higher-than-average loads at the same time as others experiencing an opposite trend – that might be potentially problematic for sectoral integration?
4. Is it possible to identify sub-national entities for which the deployment of NZEBs would provide highest load-smoothing benefits across multiple weather years?

Yet, answering such questions requires spatially- and temporally-resolved residential heat demand profiles for multiple weather years, which, for most European countries, are not available in the form of metered, empirical data. What is more, even whereas empirical data are available, those do not allow accounting for the key benefits potentially brought about by NZEBs. Therefore, several authors have proposed methods to generate bottom-up synthetic residential space-heating profiles at the country scale with the desired spatial and temporal resolutions, and for any weather year. However, none of the methods proposed so far in the literature allows to answer all the identified research questions at once. This study addresses this gap by:

1. Developing and validating an open-source bottom-up simulation workflow to generate synthetic residential space-heating profiles at high spatial (NUTS3) and temporal (1-h) resolution, including – the first of its kind – NZEB refurbishment scenarios.
2. Applying the workflow to the case of Italy, quantifying and discussing the variability of residential space-heating demand across weather years in the range 2000–2018 for various temporal and spatial scales, for both the current and an NZEB-refurbished building stock.

The paper is organised as follows. Section 2 provides a critical literature review of existing approaches to the simulation of highly resolved residential space-heating demand at the country scale. Section 3 presents the modelling approach proposed by this study, alongside all the data and the sources required by it. Section 4 provides a comparison of the proposed approach against other estimates of space heating demand and the full set of results, alongside their critical discussion.

Review of approaches to the modelling of country-scale space-heating demand.

Previous work has proposed methods to generate synthetic residential space-heating profiles at high spatial and temporal resolutions, for a given weather year. Such methods can be broadly classified into: a) *standard load profile reanalysis*; and b) *thermodynamic simulation*.

The first group consists of approaches revolving around the idea that, once a reliable “standard heat load profile” (SLP) is defined based on either existing national standards or measurements, this can be simply modulated according to the different required climatic conditions or building categories. A notable example of such an approach is represented by the *When2Heat* dataset, elaborated by Ruhnau et al. [6] combining the SLP adopted by German gas operators with meteorological conditions reanalysis and building stock information, and applied to a number of European countries – namely those deemed similar enough to the reference case in terms of climatic conditions and building types. A similar approach, though restricted to the German context, is adopted by the open-source project *demandlib* [7]. The European project *HotMaps* [8] also grounds on the definition of non-dimensional standard load profiles, though in this case referring to typical heat pump operation profiles, which are then adapted, with temperature corrections, to the whole EU. Such heat-pump-specific profiles, however, have the drawback of limited relevance for integration with energy models in which the type and operation of the heat conversion technology are subject to optimisation themselves, i.e. when heat pumps are considered as subject to smart remote control by aggregators [9]. Another open-source project, the DeSTINEE model developed by Boßman and Staffel [10], builds on the identification of a standard, non-dimensional heating profile, which is then adapted to all EU countries and made subject to random noise in any time step and day. Brown et al. [11] also adopt a combination of standard profiles gathered from the Danish city of Aarhus and country-specific daily temperature reanalyses to generate EU-wide heat demand profiles. All such approaches have the considerable advantage of being quickly adaptable to different contexts, while ensuring that the profile shape, grounded on a referenced standard, is never too far from reality. Nonetheless, as commented by Ruhnau et al. [6], adaptability is constrained by the degree of similarity, in terms of climatic conditions and associated building stock characteristics, between the reference context and any different one. What is more, the use of a SLP prevents the simulation of non-linear changes in heat demand profiles resulting from building stock refurbishment policies and NZEBs penetration, already planned in many countries as part of EU heat decarbonisation plans.

The group of *thermodynamic simulation workflows*, instead, ground on the idea of generating synthetic heat demand profiles based for a number of building archetypes, based on thermodynamic simulations of buildings' response to (at least) changes of outdoor conditions. Archetypes are then aggregated to the country scale as part of a broader workflow. Several degrees of complexities are hence possible, and at least three sub-groups can be differentiated based on the way in which the thermodynamic simulation at the core of the workflow is carried out. The sub-group featuring the simplest thermodynamic simulation approach is that in which a direct proportionality relationship is assumed between outdoor temperature and indoor comfort temperature and no distinction is made across building types. For instance, this is the approach detailed in the STRATEGO project [12], in which the heating system is assumed to be turned on in any hour of the year in which the outdoor temperature drops below 15 °C, proportionally to the difference between the latter and the indoor set point. Nonetheless, direct proportionality relationships may be inaccurate in capturing building dynamics and inertia [13] and may fall short in handling NZEBs penetration scenarios. At the other extreme of complexity, another sub-group is the one that aims at the description of a full country-wide building stock based on a restricted number of highly-detailed building archetypes, whose dynamic behaviour is accurately simulated by means of a professional building-physics software. Such an approach has been proposed, among others, by Clegg and Mancarella [14] for the simulation of hourly-resolved heat demand profiles for the UK. For the residential sector, they define four (4) possible geometries and three (3) insulation levels, and simulate each combination of these by means of the EnergyPlus software. Despite the very high accuracy ensured by the software-based thermodynamic simulation, this method is demanding in terms of data gathering, software license availability and computational effort, and might be hardly replicable and adaptable to different contexts. Finally, a third sub-group is that of lumped-parameter thermodynamic representations of the building stock. These also ground on the definition of a (typically larger) number of building archetypes, which are then simulated adopting a lumped-parameter approach, or electrical analogy [13]. The

approach is flexible, with the degree of complexity arbitrarily definable, for instance by modelling a building as a single- or multi-node equivalent circuit, allowing to set the desired balance between accuracy and computational efficiency. Such an approach has been demonstrated by Gendebien et al. [15], with application to the Belgian building stock, represented by the authors by means of up to 338′688 combinations of different building characteristics. The study also demonstrated the versatility of the method in the simulation of desired refurbishment interventions. Patteeuw et al. [16] similarly developed a lumped-parameter building stock representation of Belgium, demonstrating its potential for a hard-linked integration with power systems optimisation. A lumped-parameter model has been also proposed by Heinen et al. [17] with application to Ireland, showing how the method ensures good accuracy compared to software-based individual buildings simulations.

The bottom-up building stock lumped-parameter simulation emerges hence as a promising and versatile compromise between computational effort and building-physics accuracy, while being also suited to simulate refurbishment scenarios. Furthermore, lumped-parameter approaches allow for the quick simulation of any weather year based on the simple variation of radiation and temperature input time series. However, the workflows grounding on lumped-parameter approaches that have been proposed so far in the literature failed to ensure:

(i) repeatability, due to the adoption of closed-source code;
(ii) adaptability to other contexts, due to the large amount of data to be collected to characterise the context of interest; and
(iii) adaptability to different scales, due to the lack of sub-national disaggregation.

All features which are instead critical to answer the research questions that have been identified in Section 1. What is needed is a lumped-parameter representation of the building stock that ensures an accurate-enough representation of building dynamics based on a limited, context-adaptable set of parameters, while also allowing for the detailed simulation of refurbishment scenarios (i.e., change of insulation materials and thickness) which reflect the most recent guidelines for NZEBs. It is also crucial to have a high spatial granularity, capturing site-specific weather conditions, and different levels of spatial aggregation (regional, national, etc.) to provide outputs that are valuable for different levels of legislative authorities on building refurbishment regulation.

Building on a proof-of-concept presented in previous work [18], this work thus proposes an open-source simulation workflow that grounds on a well-established, standardised lumped-parameter thermodynamic model (the EN ISO 52016:2017 [19], as further discussed in sub-section 3.1) to simulate any building stock based on a number of parameters that compromises between adaptability to different contexts and physical accuracy. The simulation workflow, which takes the name of HeCo and is released publicly [20], includes a realistic representation of NZEBs as a refurbishment option, and allows to simulate any desired future country-wide building refurbishment plan with a spatial granularity ranging from NUTS3 to NUTS1 and hourly temporal resolution.

2. Materials and methods

The simulation workflow proposed in this paper grounds on the definition of a set of building archetypes, whose space-heating demand is computed by means of a lumped-parameter model. Fig. 1 summarises the criteria adopted for the differentiation of such building archetypes, namely: a) geometry, b) construction period, and c) climate-dependent construction materials.

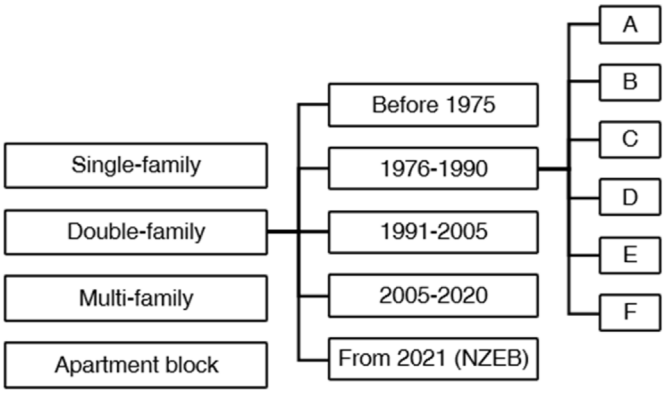

Fig. 1. Conceptual scheme of the disaggregation of building archetypes in the proposed workflow by geometry, construction period and climate-dependent construction materials.

In line with previous studies [15], four building geometries are here deemed sufficient to represent the diversity of building types existing within a country-wide building stock. These are: single-family, double-family, multifamily houses and apartment blocks. For the case of Italy, this type of macro-categorisation is also adopted by the national bureau of statistics [21]. Construction periods (influencing materials and heat transfer coefficients) are instead defined according to the evolution of the national legislation for the context of interest. For Italy, the key historical regulations on buildings suggest discriminating between buildings constructed: before 1975; from 1976 to 1990; from 1991 to 2005; and from 2006 to 2020. To these, a fifth construction period corresponding to NZEBs is added, considering that the Energy Performance of Buildings Directive [22] requires all private buildings constructed after December 31st' 2020 to comply with NZEB regulations. Finally, different climate-dependent groups of construction materials are considered, to reflect the fact that areas characterised by different regional climates, within the same country, typically adopt different building techniques and materials. Italy comprises six different climatic areas (from A, the warmest, to F, the coldest), and one macro-category of construction materials for each is hence defined. The combination of all such options, easily adaptable to a different country case, provides a total figure of 120 different building archetypes.

2.1. Thermodynamic formulation of a building archetype

In this work, the thermal behaviour of an individual building archetype is represented by means of a resistance-capacitance (RC) lumped-parameter model provided with two capacitances. Such capacitances refer to the internal ambient and to the building elements. Compared to single-capacitance models, this ensures a good accuracy for both winter and summer thermal dynamics (i.e., heating and cooling), as discussed by Vivian et al. [13]. In particular, our RC model grounds on that defined in the EN ISO 52016:2017 [19], adopted also by Ramallo-González et al. [23]. Each building is modelled as a box-shaped single heated/cooled thermal zone and is assumed to be composed by 10 building elements: the roof, the floor and the four vertical walls differentiated by transparent and opaque surfaces, as shown in Fig. 2 a.

The explicit thermodynamic equations summarised by the lumped-parameter model applied in this work are: the energy balance on the external surface of each building element (Equation (1)); the energy balance on the internal surface of each building

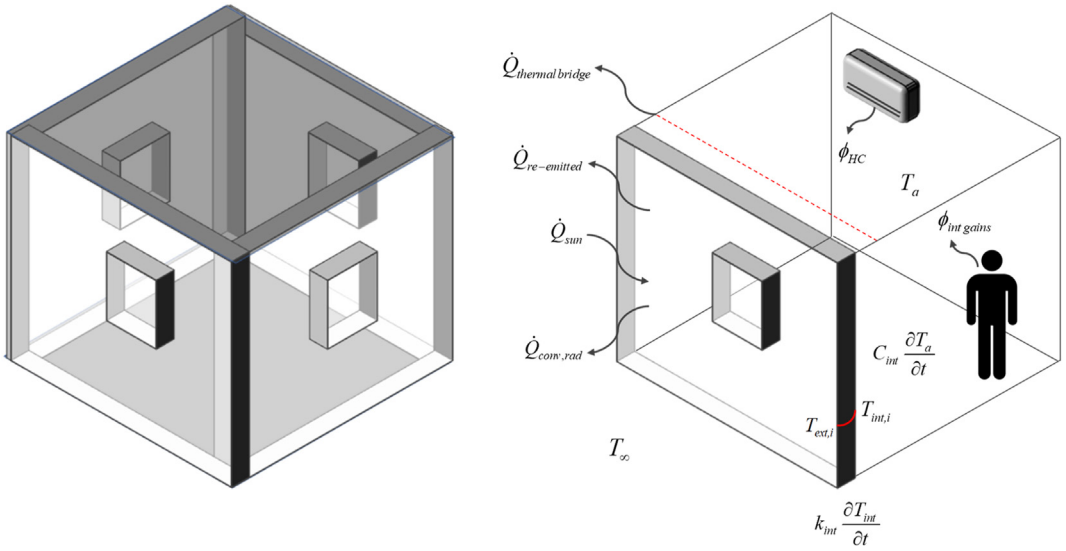

Fig. 2. Schematic representation of an archetype and of its main thermodynamic variables. Panel **a** shows the box-shaped single thermal zone archetype representation adopted, with the resulting 10 building elements (roof, floor, 4 walls, 4 windows). Panel **b** shows instead the main variables and heat flows characterising the thermodynamic problem for such kind of building archetype.

element (Equation (2)); and the overall energy balance of the thermal zone (Equation (3)). Such equations are derived, as anticipated, from the well-established ISO 52016:2017 [19], though with the application of the following simplifications, which facilitate the application of the model for thousands of buildings within the proposed country-wide simulation workflow: i) mechanical ventilation appliances are neglected, since those are not widespread among residential buildings; ii) each building element is modelled as a conductive resistance coupled with a capacitance applied to the node facing the internal volume; iii) transparent building elements are assumed to have null capacitance.

$$(h_{se}+h_{eli})T_{ext,eli,t}-h_{eli}T_{int,eli,t}=h_{se}T_{e,t}+a_{sol}\left(I_{diff,eli,t}+I_{dir,eli,t}F_{sh,eli}\right)-\phi_{sky} \tag{1}$$

$$-(h_{eli}T_{ext,eli,t})+\left[\frac{\kappa_{pli,eli}}{\Delta T}+h_{ci,eli}+h_{eli}\right]T_{int,eli,t}-h_{ci,eli}T_{a,t}=\frac{\kappa_{pli,eli}}{\Delta T}T_{int,eli,t-1}+\frac{1}{A_{tot}}\left[(1-f_{int})\Phi_{int,t}+(1-f_{sol})\Phi_{sol}+(1-f_{HC})\Phi_{HC,t}\right] \tag{2}$$

$$\left[\frac{C_{int}}{\Delta t}+\sum_{eli=1}^{eln}(A_{eli}h_{ci,eli})+H_{ve}+H_{tr}\right]T_{a,t}-\sum_{eli=1}^{eln}(A_{eli}h_{ci,eli})T_{int,eli,t}=\frac{C_{int}}{\Delta t}T_{a,t-1}+(H_{ve}+H_{tr})T_{e,t}+f_{int}\Phi_{int,t}+f_{sol}\Phi_{sol,t}+f_{HC}\Phi_{HC,t} \tag{3}$$

where h_{eli}, h_{se}, $h_{ci,eli}$, H_{ve} and H_{tr} are the heat transfer coefficients; $I_{diff,eli,t}$ and $I_{dir,eli,t}$ are the solar irradiances; C_{int} and $\kappa_{pli,eli}$ are, respectively, the two capacitances of the internal ambient and building element i; $T_{a,t}$, $T_{e,t}$, $T_{int,eli,t}$ and $T_{ext,eli,t}$ are, respectively, the internal and external ambient temperature and the internal and external surface temperature of the ith building element; and $\Phi_{int,t}$, $\Phi_{sol,t}$ and $\Phi_{HC,t}$ are the heat gains provided, respectively, by internal elements (inhabitants and appliances), direct sun radiation and the heating and cooling system. Fig. 2 b summarises the thermodynamic problem and the main variables at stake. All thermophysical parameters required to populate each modelled archetype are derived from ISO standards and existing national or European projects. A more exhaustive discussion of such variables and parameters, including data sources, is provided in Appendix B.

2.2. Control logic and spatial aggregation

The lumped-parameter model is packaged into a broader simulation workflow, implemented in a Python 3.6 environment and solved for each building archetype in each NUTS3 Italian region, with its related location-specific climate-dependent construction materials and weather data (for the desired weather year). As summarised in Fig. 3, once the comfort indoor temperature set points for the cold and hot season are defined, the lumped-parameter model can be solved in hourly timesteps to compute: i) the ambient temperature change in the given timestep as a function of boundary conditions, e.g. when the heating/cooling system is off; or ii) the heating/cooling load needed to meet the predefined comfort ambient temperature in a timestep in which boundary conditions require the system to be switched on.

The algorithm is also constrained to follow approximated real-life user dynamics and Italian normative prescriptions. First, the workflow defines for each climate zone the precise period in which residential heating is allowed by the Italian legislation (Table 5). Second, it defines three different possible indoor daily thermostat regulation settings (or *user types*), which correspond to the most typical daily regulation settings among Italian households (Table 6) [24]. In each location, the workflow simulates 1/1000 of all real dwellings, and it variates regulation settings among all simulated dwellings proportionally to user type share in that given location [21], as reported in the Appendix B. Results at NUTS3 resolution can be hence further aggregated at need to provide NUTS2- or NUTS1-resolution outputs.

2.3. Specific features of nearly zero-energy buildings

A key peculiarity of the proposed workflow is its capability of simulating refurbishment scenarios, in which older buildings are renovated according to NZEB regulations. As such, the workflow

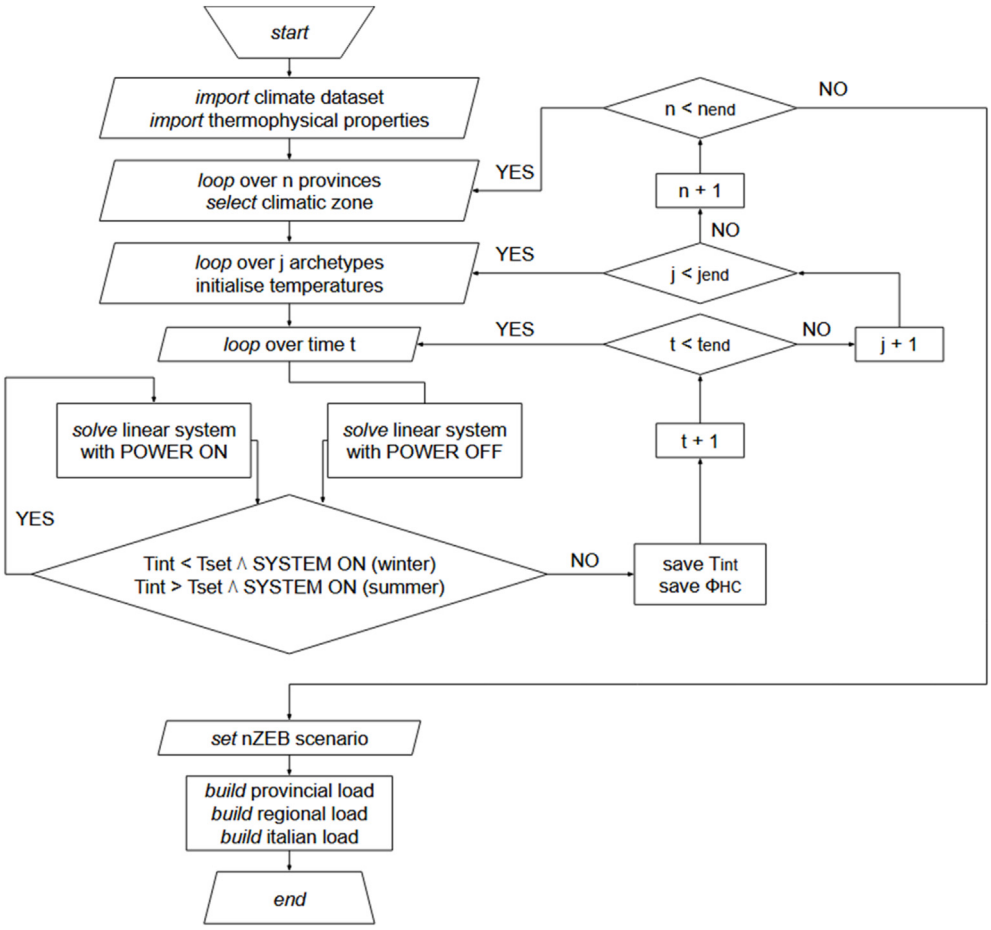

Fig. 3. Conceptual flow chart summarising the simulation workflow logic. In each timestep, the algorithm computes the building's thermodynamic properties assuming no heating/cooling load. If the resulting internal temperature is lower (or, respectively, higher for the case of cooling) than the set point, the thermal balance is re-computed in order to obtain the heating (or, respectively, cooling) load required to meet the set point temperature. Otherwise, the algorithm proceeds to the subsequent timestep. The workflow iterates over each province (i.e., NUTS3 region), accounting for building and climate characteristics of each.

implements formal criteria for the refurbishment of older buildings into NZEB within the adopted lumped-parameter approach. In particular, it is assumed that existing buildings can be turned into NZEBs by improving their insulation characteristics by means of an ad-hoc envelope and by applying radiation shielding to windows. It is worth noting that, considering the focus on demand of the present work, NZEB prescriptions related to the more efficient energy appliances are here neglected. To identify the exact value by which existing buildings properties, and particularly the envelope characteristics, need to be improved in order to be classified as NZEB, our workflow relies on prescriptions from the 2015 Italian legislation on the matter [25]. More precisely, the workflow identifies the maximum transmittance (U-values) admitted for each building element of a renovated house to be considered NZEB — with each climatic zone having its own specific U-value limits. For the new archetypes, all transmittance values are assumed equal to the minimum (i.e., the most binding) values admitted by the NZEB definition. The relationship between U-values and the parameters in thermodynamic model is reported in Equation (5), while Table 7 reports the assumed U-values for the NZEB archetypes.

2.4. Refurbishment scenarios

The present analysis considers two building stock scenarios. First, a "*Business as Usual*" (BAU) scenario, which simulates the building stock in its present state (or, more precisely, in 2011, to which the most recent building stock census dates back). Second, a scenario which simulates the penetration of NZEBs in Italy as forecasted by the European project ZEBRA2020 (and hence named for simplicity the "*ZEBRA2020*" scenario). The developed workflow simulates refurbishment policies by assuming that older and more energy-intensive buildings (those constructed before 1975), which also represent the largest share of the current building stock, are those renovated first. The ZEBRA2020 project estimates a 35% penetration of NZEBS in Italy by 2030, which means, based on the aforementioned rationale, that 54.77% of all buildings constructed before 1975 is refurbished, whilst those from more recent periods remain untouched.

3. Results and discussion

This section discusses the accuracy of the HeCo simulation workflow and summarises the main outcomes of its application, with a focus on the analysis of the temporal and spatial variability of heating and cooling profiles generated for the two above-mentioned scenarios.

3.1. Model comparison against other estimates

In the absence of metered hourly data at the country scale, the model is compared against estimates of yearly space heating consumption by Eurostat [26], available for years in the range

2015–2018, and When2Heat [6], available for years in the range 2008–2013. Raw data from Eurostat refer to final energy consumption; to obtain useful energy consumption figures, as simulated by the HeCo workflow and by When2Heat, a conversion factor of 0.9 is applied, in agreement with Ruhnau et al. [6]. Data for cooling yearly consumption are also available from Eurostat, but several dwellings equipped with cooling systems declare they use it only occasionally, irrespective of the theoretical set point assumed for cooling activation, and often only for a restricted number of rooms in the house, making a comparison problematic. Therefore, the present comparison focuses on space heating data, whilst simulated cooling loads can be regarded as maxima theoretical loads, for which households use cooling systems based on a purely thermostatic control logic, and to cool the entire house. Table 2 shows how, for the available range of data, the model provides a higher estimation of the yearly total space heating demand compared to the other existing estimates, with percentage deviations ranging between 15% and 27%, except for the year 2018. It is worth considering, to this regard, that the building-stock information adopted for the study (grounded on a 2011 census) become less accurate for most recent years, in which an increasing number of buildings has been refurbished compared to the reference database. In general, the higher estimation compared to other sources, which ground on surveyed information, can be also attributed to the simplifications introduced in the workflow compared to real-life conditions, such as the restricted number of possible user behaviours. It is worth noting, however, that even the datasets chosen for comparison represent themselves only *estimates* of useful residential space-heating demand, and that no metered, fully reliable dataset exists.

Appendix A reports also a test of the sensitivity of model results to variations in key uncertain parameters, such as the assumed shading factor on each simulated building and the user thermal comfort settings. The model demonstrates limited sensitivity to even large variations of assumptions regarding the shading factor, and a negligible sensitivity to the randomisation of comfort setting preferences in a realistic neighbourhood of typical values.

3.2. Space heating and cooling profiles

Fig. 4 provides an overall picture of the temporal variability, throughout the year, of the aggregate space heating and cooling profiles for the entire Italy, across the full range of simulated weather years and for the two refurbishment scenarios considered. As expected, refurbishment policies do not significantly alter the overall cooling load. During warm months, there is a trade-off between reduced window transmittance and increased insulation, producing an overall negligible change in cooling loads compared to those of buildings constructed after 2005. Furthermore, cooling demand profiles show limited variability across weather regimes. On the contrary, the influence of the weather on the space heating load is clearly visible, with unfavourable weather years provoking peaks in the daily space heating profile up to 2 TWh/day higher than for typical conditions, and with a duration of several days. To this regard, the renovation of the building stock ensured by the ZEBRA2020 scenario leads to significant absolute reductions (31–37% depending on the weather year) in the space heating loads and, consequently, in the absolute extent of such weather-induced fluctuations.

Notably, as shown in the inset of Fig. 4, weather-induced variations are relevant not only at the daily temporal scale, but also as regards hour-by-hour dynamics. In particular, the load between morning and evening peaks experiences remarkable fluctuations across different weather regimes. If these dynamics were to be directly translated into an electrical load by resistive heating, they would likely exacerbate ramping issues within the power system. Again, NZEBs penetration in the building stock produces absolute reductions in such steep fluctuations, even though the behaviour of the profiles remains subject to weather-induced hourly variations. This suggests that, while the impact of NZEBs is remarkable in terms of absolute demand reduction, other measures should be coupled with refurbishment to better tackle intra-day fluctuations. Future studies should investigate, in combination with a power system model, if and to what extent such intra-day fluctuations could be further mitigated by the adoption of heat pumps coupled with thermal storages and smartly interacting with power system signals.

These results provide some insights about the first two research questions identified in Section 1. 1. In fact, it is possible to conclude that, first, country-wide residential space-heating demand can vary markedly across weather years, both at the temporal scale of days (e.g., as shown by the several-day demand peaks experienced over only in a few weather years in February, in Fig. 4) and at the scale of hours, as just discussed. Second, while NZEBs would have a positive effect by ensuring absolute reductions of heat demand that would limit the relevance of prolonged unfavourable weather conditions, they would not be able to address issues associated with weather regimes that generate marked intra-day demand variability. A similar result could not have been attained by means of existing approaches (see Table 1), since none of those would've allowed a physically accurate accounting of NZEB penetration for thousands of buildings aggregated up to the country scale while ensuring computational tractability.

3.3. Spatial asymmetries across weather years

The total yearly demand for space heating exhibits marked variability also from a spatial perspective. Fig. 5 shows, for each Italian region, the relative deviation of yearly space heating

Table 1
Notable examples of country-wide heat demand simulation models and approaches in the literature, and their potential to take into account weather-induced demand variations across weather years.

Model type	Standard load profile (SLP) reanalysis	Thermodynamic simulation		
		Direct proportionality	Software-based	Lumped-parameter
Examples in the literature	When2Heat [6] Demandlib [7] HotMaps [8] DeSTINEE [10] Brown et al. [11]	STRATEGO [12]	Clegg and Mancarella [14]	Gendebien et al. [15] Patteeuw et al. [16] Heine et al. [17]
Possibility to account for weather year variations	No/constrained to few weather years	Yes	Yes (but computationally burdensome)	Yes
Possibility to account for refurbishment	Limited to absolute yearly demand reduction	Limited to absolute yearly demand reduction	Yes (but computationally burdensome)	Yes

Table 2
Percentage relative difference between yearly residential space heating demand simulated by HeCo and estimates from other sources, for different weather years. The year 2014 is missing due to no dataset covering it.

Source\Year	2008	2009	2010	2011	2012	2013	2015	2016	2017	2018
Eurostat	–	–	–	–	–	–	26.7	24.4	27.1	32.5
When2Heat	15.1	16.7	26.7	24.1	19.1	22.8	–	–	–	–

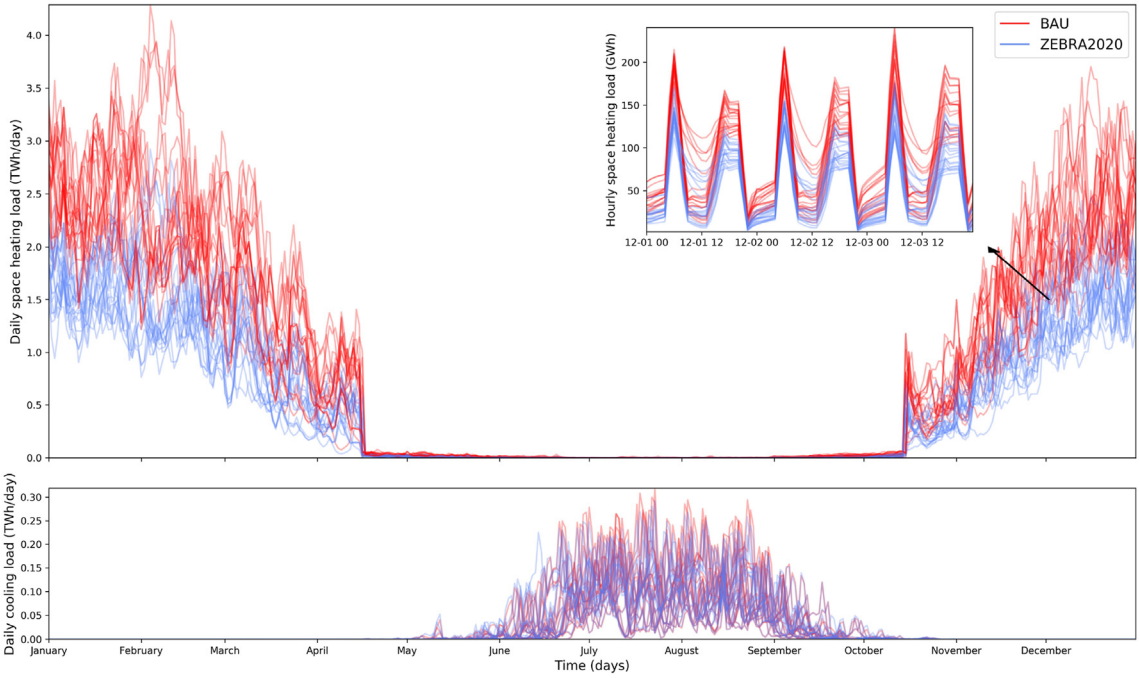

Fig. 4. Space heating (top) and space cooling (bottom) energy demand aggregated for the entire Italy. The main plots show daily consumption (TWh/day) throughout the year, and across the full range of considered weather years, for the BAU and the ZEBRA2020 scenarios. The inset shows a magnification of the main plots for a representative week in December, in which profiles are represented at hourly resolution. It is worth noting that in the period April 15th – October 15th only buildings belonging to climatic zone F are allowed to use space heating, based on Italian legislation; yet, inasmuch as such buildings represent a very small fraction of the total, their space heating demand is barely visible in the figure.

demand each year with respect to the average demand calculated across all weather years for the same region. Whilst some weather years entail a relatively homogeneous behaviour across regions, i.e., an overall reduction or increase in space heating demand throughout the country, others lead to spatially asymmetric conditions. For instance, the weather year 2003 leads to an asymmetric behaviour between northern and central-southern regions, in which the North faces lower-than-average heat demand whilst the Centre and the South need to cope with higher-than-average demand. On the contrary, the weather year 2010 entails extremely unfavourable deviations from average space heating demand for many northern regions, whilst southern ones experience only moderate deviations. All such asymmetric conditions raise possible challenges in terms of space heating electrification and integration with renewable power. In particular, it is worth noting that, in absolute terms, demand for space heating in the North is much larger due to a larger population (and number of dwellings) in addition to a colder climate, whilst several large renewable power plants are located farther South. Hence, conditions like those experienced in 2010 may be particularly problematic for system regulation.

This answers the third research question identified in Section 1: there can be asymmetries in the variability of heat demand at the sub-national scale, and those shall be explicitly taken into consideration with particular care when designing sector-coupled energy systems, avoiding to design systems based on typical conditions only. Again, this highlights the urgency of studying simultaneously heat demand and renewable power fluctuations within power system models, in such a way to: i) identify renewable and transmission capacity expansion plans that are able to cope with critical spatial asymmetries of this kind; and ii) assess whether the absolute reductions in heat load ensured by NZEBs can mitigate the relative impact of such asymmetries to an extent that weather-tailored capacity expansion plans become unnecessary. The developed HeCo workflow makes these studies finally possible, overcoming the lack of sub-national detail and of NZEB features which characterised existing approaches.

3.4. Region-specific impact of nearly zero-energy buildings

The absolute reduction in peak and total yearly heat demand ensured by NZEBs is, of course, strongly driven by the population and number of dwellings in each region. In fact, Lombardia is the region showcasing the highest absolute benefits from NZEB penetration. However, other factors play a role in NZEBs impact on heat demand, such as the type and construction period of renovated buildings, which varies across regions, and climatic conditions. To this regard, Fig. 6 shows how the impact of NZEBs penetration on the heat load duration curve is not spatially uniform. The relative change in the load distribution is indeed much less pronounced for southern or island regions, such as Sardegna, Sicilia and Puglia, characterised by warmer climate and higher solar radiation.

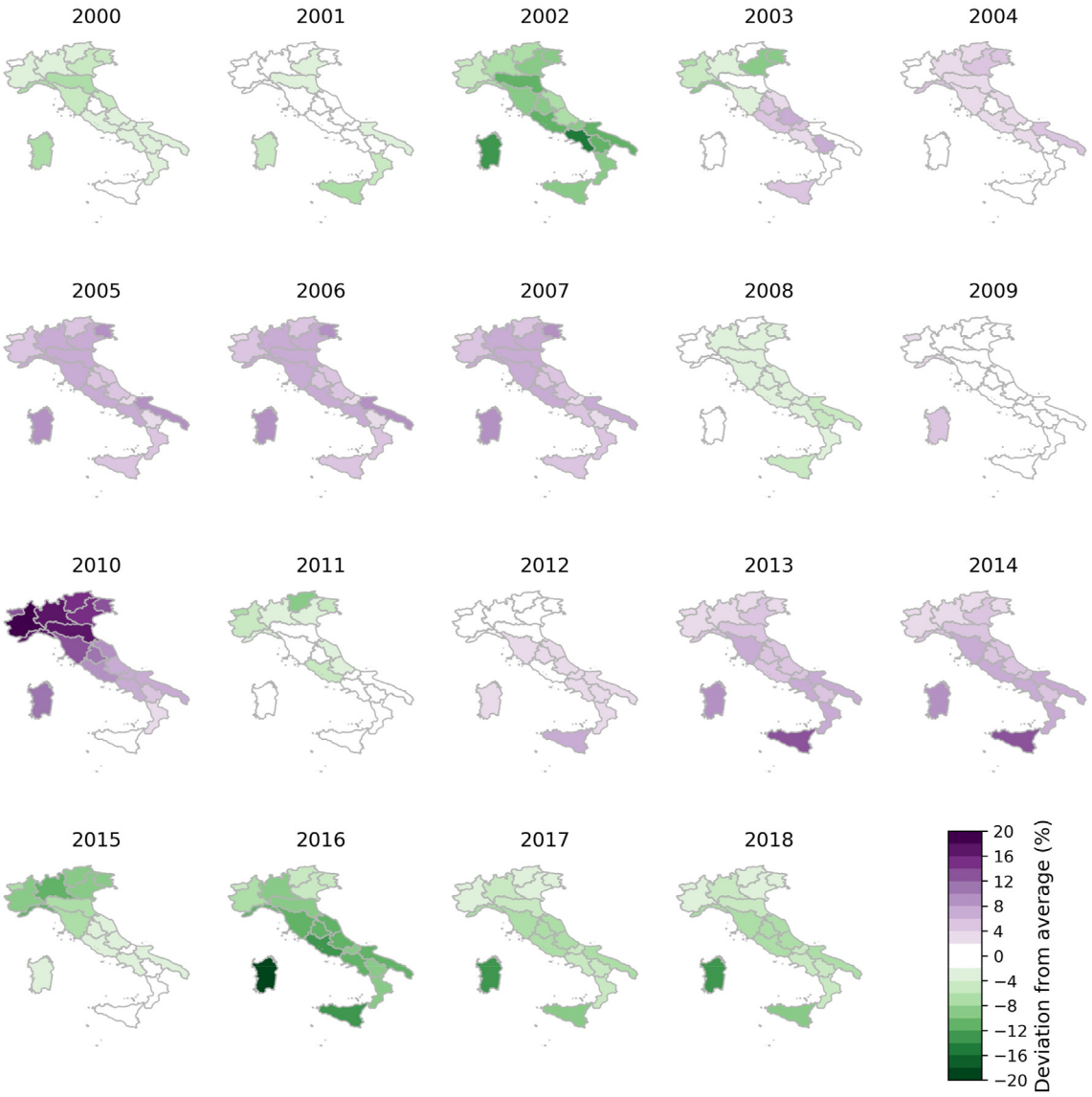

Fig. 5. Region-by-region percentage deviation of total regional yearly space heating demand, for a specific weather year, with respect to the regional yearly average across all considered weather years.

Amongst northern regions, instead, Piemonte and Valle d'Aosta stand out as particularly benefitting from NZEB refurbishment, with a load duration curve showing the most marked relative decrease. Overall, NZEB penetration seem to smooth out mostly high and medium-high load demand, with a less-marked effect on baseload. This is also a consequence of the fact that, frequently, the improved insulation ensured by NZEB makes a given heating switch-on event entirely unnecessary when it was previously needed, therefore reducing the number of coincident loads in a region and hence the peak total load.

Answering the fourth and final of the research questions presented in Section 1, these results confirm that it is indeed possible to identify sub-national entities for which the deployment of NZEBs would provide highest load-smoothing benefits across different weather regimes. This is an additional benefit of modelling space-heating demand with both a high spatial and temporal resolution and a detailed characterisation of the building stock. Unlike for previous approaches, it is possible to identify regions in which refurbishment interventions shall be prioritised, such as Piemonte and Valle d'Aosta, and those in which the energy policy budget might be better redirected towards other needs.

4. Conclusions

This work presented and validated first-of-its-kind, open-source workflow for the simulation of space-heating demand at the country scale with high temporal resolution and sub-national disaggregation. The workflow, which grounds on a well-established lumped-parameter model for the simulation of individual building archetypes that are subsequently aggregated bottom-up, compromises between thermodynamic accuracy and easiness of data gathering for any context of interest. The workflow provides slightly higher estimates of total yearly demand compared to other existing estimates, yet proves particularly useful and unique in its capability of simulating any future refurbishment scenario, particularly the renovation of old buildings according to NZEB regulations, and of accounting for sub-national demand asymmetries.

The application of the model to the Italian case across weather years in the range 2000–2018 shows that:

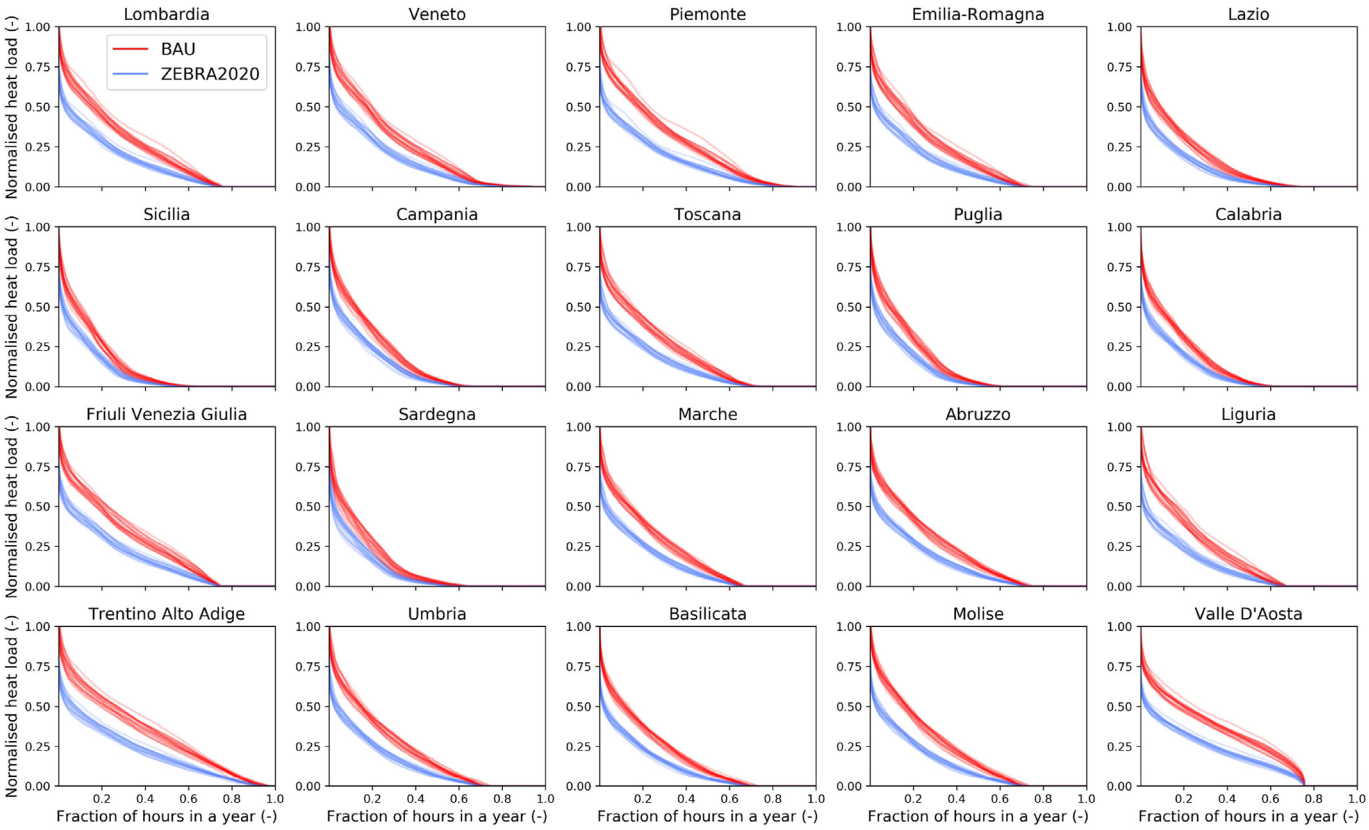

Fig. 6. Load duration curve related to the normalised space heating load demand in each Italian region, for BAU and ZEBRA2020 scenarios. The normalisation is performed with respect to the highest peak value across all scenarios and weather years in each region. Timesteps in which the legislation prescribes that the heating system be turned off have been cut from the load duration curve representation to obtain a clearer visualization of other months.

1. Different weather regimes can produce steep fluctuations in total and peak space-heating demand, which can last for several days. Moreover, they can also entail marked intra-day fluctuations.
2. Particularly unfavourable weather regimes also entail spatial asymmetries that may stress transmission bottlenecks across the peninsula and make renewable generation far from point of consumption risky. Sectoral-integration studies should take such conditions explicitly into account to avoid a system design that is not fit to cope with other-than-typical weather regimes.
3. A realistic penetration of NZEBs, aligned with the forecasts of the ZEBRA2020 project, does provide significant absolute reductions in heat demand, as well as in absolute weather-induced fluctuations. In particular, NZEBs appear as a key technology to mitigate the large weather-induced fluctuations which occur over a time-span of several days, whilst less so when it comes to mitigating intra-day demand peaks, which are primarily driven by user control logics. As such, it is critical to couple future refurbishment policies with others aimed at fostering the penetration of smart heat generation technologies equipped with thermal storage in all renovated buildings, in such a way to further smooth out intra-day hourly heat demand fluctuations.
4. It is possible to identify regions for which the impact of NZEB would be highest. For Italy, Northern regions seem to potentially benefit the most from NZEB penetration, both from an absolute and a relative perspective.

Modelling heat demand with spatial, temporal and thermo-physical (including NZEB features) detail is critical to capture the abovementioned phenomena, which previous approaches did not allow. The developed workflow makes possible, for future energy system planning studies, to simultaneously account for weather effects on both renewables and heat loads at high spatial and temporal detail, as well as to explicitly test or optimise system design across all weather regimes, including particularly unfavourable ones. This will be a key next step to provide further insights about which additional measures, besides NZEBs, should be put in place on the power-system side to allow for a frictionless integration of power generation and space-heat supply.

While the model is already capable of providing timely policy insights, it has scope for further enhancement. The computational performance might be further improvement by means of systematic code profiling, in such a way to allow the inclusion of additional load diversity elements, such as, for instance, the simulation of a wider set of user behaviour types, which might mitigate the risk of excessive coincident behaviour and hence of peak demand overestimation. To this regard, it might be worth trying to expand model testing in the direction of hour-by-hour dynamics by looking for metered data from large-enough utilities and/or private companies in Italy and beyond. Large utility data would allow obtaining, if not a full country-wide hour-by-hour dataset for comparison, at least a temporally-resolved dataset of thousands of independent users, from which aggregate hourly demand dynamics could be appreciated and used for additional model testing and refining. Furthermore, it would be important to improve the representation of cooling loads by means of more detailed statistical information about the building-area coverage (i.e., only one room, all rooms, etc.) and

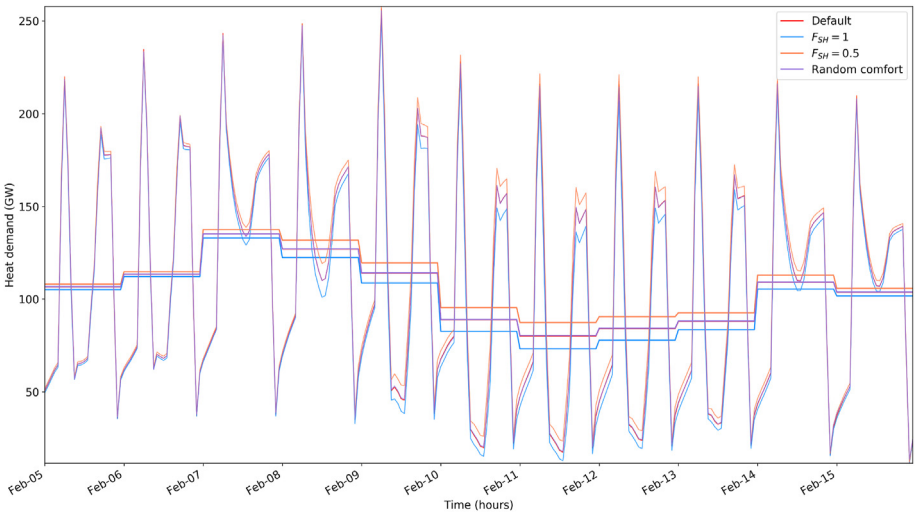

Fig. 7. Sensitivity of model results to variations of uncertain parameters for a representative 10-day period in February (2015 weather data). The figure shows both the hourly profiles and the daily average heat demand for Italy as a whole, for each sensitivity scenario and for the default model settings.

Table 3
Sensitivity of model results to variation of the shading reduction factor.

	Default setting	$F_{SH} = 0.5$	$F_{SH} = 1$	Random comfort settings
Heat demand (TWh/year)	291.2	308.7	274.4	291.9
Err%	–	6.0%	−5.8%	0.2%

the usage behaviour preferences of existing cooling appliances. Finally, since the model is conceived for integration within larger-scope modelling frameworks, particularly power system models, a critical further development will be the realisation of such integration, which will allow the investigation of more complex interactions and phenomena, such as those outlined in the previous paragraphs.

Credit author statement

Francesco Lombardi: Conceptualization; Formal analysis; Investigation; Methodology; Project administration; Software; Validation; Visualization; Writing - original draft, review & editing. Matteo Vincenzo Rocco: Conceptualization; Methodology; Project administration; Writing - review & editing; Supervision. Lorenzo Belussi: Conceptualization; Data curation; Formal analysis; Methodology; Resources; Writing - review & editing; Supervision. Ludovico Danza: Conceptualization; Data curation; Formal analysis; Methodology; Resources; Writing - review & editing; Supervision. Chiara Magni: Conceptualization; Data curation; Formal analysis; Investigation; Methodology; Resources; Software; Visualization; Writing - original draft, review & editing. Emanuela Colombo: Conceptualization; Writing - review & editing; Supervision.

Table 4
U-values ($W \cdot m^{-2} \cdot K^{-1}$) for single-family buildings, by construction period, climatic zone and building element.

Before 1975	A	B	C	D	E	F
Vertical Walls	1.76	1.76	1.50	1.50	1.36	1.36
Roof	1.74	1.74	1.74	1.74	1.74	1.74
Floor	1.61	1.61	1.61	1.61	1.61	1.61
Transparent Elements	5.00	5.00	4.60	4.60	4.60	4.60
1976–1990	**A**	**B**	**C**	**D**	**E**	**F**
Vertical Walls	1.10	1.10	0.94	0.94	0.68	0.68
Roof	1.46	1.46	1.46	1.46	0.98	0.98
Floor	1.25	1.25	1.25	1.25	1.25	1.25
Transparent Elements	5.00	5.00	3.20	3.20	3.20	3.20
1991–2005	**A**	**B**	**C**	**D**	**E**	**F**
Vertical Walls	0.67	0.67	0.67	0.67	0.63	0.63
Roof	1.10	1.10	1.10	1.10	0.74	0.74
Floor	1.18	1.18	1.00	1.00	0.82	0.82
Transparent Elements	5.00	5.00	3.20	3.20	3.20	3.20
2006–2020	**A**	**B**	**C**	**D**	**E**	**F**
Vertical Walls	0.60	0.60	0.41	0.41	0.35	0.35
Roof	0.38	0.38	0.35	0.35	0.31	0.31
Floor	0.62	0.62	0.40	0.40	0.34	0.34
Transparent Elements	4.00	4.00	2.60	2.60	2.20	2.20

Table 5
Heating periods defined by the Italian legislation, per climatic zone.

Climatic zone	Start Date	End Date
A	December 1st	March 15th
B	December 1st	March 15th
C	November 15th	March 31st
D	November 1st	April 15th
E	October 15th	April 15th
F	(No limitations)	

Table 6
Thermostat regulation settings for different user types.

Setting	Typical user	Weekdays	Weekends
R1	Elderly People	High set point all day	High set point all day
R2	Young couple with children	Low set point from 09:00 to 16:00	High set point all day
R3	Adult couple with teenagers	Low set point from 09:00 to 18:00	High set point all day

Table 7
U-values ($W \cdot m^{-2} \cdot K^{-1}$) for single-family buildings, by construction period, climatic zone and building element.

nZEB	A	B	C	D	E	F
Vertical Walls	0.43	0.43	0.34	0.29	0.26	0.24
Roof	0.35	0.35	0.33	0.26	0.22	0.20
Floor	0.44	0.44	0.38	0.29	0.26	0.24
Transparent Elements	3.00	3.00	2.20	1.80	1.40	1.10

Table 8
Thickness (cm) of fiberglass insulation to reach nZEB status, by climatic area and construction period.

	A	B	C	D	E	F
b.1975	6.7	6.7	8.6	10.6	11.8	13.0
1976–1990	5.4	5.4	7.1	9.1	9.0	10.2
1991–2005	3.2	3.2	5.5	7.4	8.5	9.8
2006–2020	2.5	2.5	1.8	3.7	3.8	5.0

Declaration of competing interest

The authors declare that they have no known competing financial interests or personal relationships that could have appeared to influence the work reported in this paper.

Acknowledgements

The authors would like to acknowledge the contribution of Simone Locatelli to the first prototyping of the Python code which served as a basis for the HeCo simulation workflow code developed in this work.

Appendix A. Model sensitivity

The model is tested in terms of results sensitivity to key uncertain parameters, namely: a) the shading reduction factor; and b) indoor thermal comfort settings.

The shading reduction factor F_{sh} represents the ratio between the actual and theoretical direct irradiance on a building element, which can range between 0 and 1 – corresponding, respectively, to 'null' and 'complete' direct irradiance. Its assessment is highly building-specific, as it depends on detailed geometrical data on the building itself and on nearby obstacles, making it virtually impossible to compute a single average value for large-scale aggregates. The analysis is carried out for an average value of 0.75. This based on data from an analysis carried out for a generic building in Turin, under assumptions that are typical for an urban context. Nonetheless, possible deviations from this value are also identified in the range 0.50–1, and used to carry out the sensitivity analysis.

As regards thermal comfort settings, the sensitivity is performed by allowing, for each simulated building, a randomisation of the indoor comfort temperature around the typical values assumed by default. More precisely, it is assumed that users may customise the set point for indoor comfort temperature during the heating period in a ±0.5 °C neighbourhood of the typical value (20 °C). A slightly larger deviation (±1 °C) is deemed plausible, instead, for the night set point (16 °C) in the heating season and for the cooling set point (26 °C).

The sensitivity is performed for the weather year 2015. In fact, as briefly discussed in sub-section 3.1, this is the first year for which the model comparison against Eurostat data is made possible and, also, the most reliable considering that building-stock data come from a 2011 census and that the more the comparison datasets moves away temporally from 2011 the less the comparison is meaningful. As shown in Table 3, the sensitivity demonstrates a good model robustness (with maximum percentage deviation around 6%) to large variations in the assumed shading reduction factor. The sensitivity to randomised comfort settings is instead substantially negligible. Indeed, the visual representation of heat demand profiles for a representative 10-day period (Fig. 7) shows essentially an overlap between default-setting and random-comfort-setting model results. Shading factor assumptions, instead, determine slightly more visible profile modifications. However, such changes are visible only for days in which solar radiation becomes an important contribution in the thermal balance of buildings, whilst they are again negligible in all cases in which solar radiation does not represent an important contribution.

Appendix B. Additional model details

The parameters featuring in the equations that define the adopted lumped-parameter thermodynamic model (sub-section 2.1) are here discussed in greater detail, including sources from which numerical values are gathered.

B.1 Thermodynamic parameters

This sub-section focuses on those parameters associated with the thermodynamic aspects of the simulation of space heating demand, such as heat transfer coefficients, temperature and radiation data, thermal capacities, heat fluxes and dimensionless factors required in heat-transfer equations.

B.1.1 Heat transfer coefficients

The heat transfer coefficients featuring equations (1)–(3) are obtained as follows.

h_{eli} – Conductive Heat Transfer Coefficient. Each building element of the system has a specific conductive heat transfer coefficient which depends on the materials adopted and on the number of material layers. Such coefficient is evaluated as a function of the U-value (the thermal transmittance of the building element, expressed in $W \cdot m^{-2} \cdot K^{-1}$ computed as per Equation (5), based on the prescriptions of UNI EN ISO 6946:2018 [27].

$$U = \frac{1}{\frac{1}{h_{si,eli}} + \frac{1}{h_{eli}} + \frac{1}{h_{se}}} \left[W \cdot m^{-2} \cdot K^{-1} \right] \tag{4}$$

where h_{eli} ($W \cdot m^{-2} \cdot K^{-1}$) is the internal surface heat transfer coefficient; and h_{se} ($W \cdot m^{-2} \cdot K^{-1}$) is the external surface heat transfer coefficient. The first comprises both convective and radiative heat transfer coefficients and is a constant. The second assumes different values based on the direction (vertical/horizontal) of the thermal flow. Both are gathered from ISO 13789:2017 [28].

U-values for the case of a single-family building are reported in Table 4. For full numerical values, the reader is referred to HeCo's open repository.

H_{ve} – **Overall Heat Exchange Coefficient by Ventilation**. As described in ISO 52016–1:2017 [29], such coefficient is computed as per Equation (6).

$$H_{ve} = \rho_a c_a q_{V,t} \left[W \cdot K^{-1} \right] \tag{5}$$

where the product $\rho_a c_a$ ($J \cdot m^{-3} \cdot K^{-1}$) is the heat capacity of air per unit volume; and $q_{V,t}$ ($m^3 \cdot s^{-1}$) is the airflow rate.

H_{tb} – **Overall Heat Transfer Coefficient for Thermal Bridges**. Again based on in ISO 52016–1:2017 [29], this coefficient is computed as per Equation (7).

$$H_{tb} = \sum_k \left(l_{tb,k} \cdot \psi_{tb,k}\right) \left[W \cdot K^{-1}\right] \quad (6)$$

where $l_{tb,k}$ (m) is the length of a linear thermal bridge k; and $\psi_{tb,k}$ ($W \cdot m^{-1} \cdot K^{-1}$)) is the linear thermal transmittance of a linear thermal bridge k, both obtained from ISO 13789:2017 [28].

Buildings constructed after 2005 represent an exception; for such category, H_{tb} is assumed equal to a 15% increase of the overall heat transfer value due to transmission, as fixed by D. lgs n.192/2005 [25].

B.1.2 Weather data

All weather data (outdoor ambient air temperature, and diffuse and direct radiation for different surface orientations) are gathered from Renewables. ninja, an openly accessible database which provides weather data and renewable generation patterns for any location in the world, based on the weather reanalysis methodologies proposed by Pfenninger & Staffel [30].

B.1.3 Thermal capacities

Thermal capacities featuring equations (2) and (3) are obtained as described below.

***$k_{int,eli}$* – Internal Areal Heat Capacity of the Building Element**. The internal areal heat capacity is calculated with a simplified method as a product of the thickness of the wall, the density and the specific heat of the material, based on the prescriptions of ISO 52016–1:2017 [29].

***C_{int}* – Internal Thermal Capacity**. The thermal capacity of the internal environment is computed according to ISO 52016:2017 [29], by means of Equation (8).

$$C_{int} = k_{int} A_f \left[J \cdot K^{-1}\right] \quad (7)$$

where k_{int} ($J \cdot m^{-2} \cdot K^{-1}$) is the areal thermal capacity of air and furniture of the considered building; and A_f (m^2) is the useful floor area of the building.

B.1.4 Heat fluxes

Heat fluxes featuring equations (1)–(3) are obtained as described below.

***Φ_{int}* – Total Internal Heat Gain**. Following the prescriptions of UNI/TS-11300–1:2014 [31], the total internal heat gains are computed as a function of the total floor area, as per Equation (9).

$$\Phi_{int} = 7.987 \cdot A_f - 0.0353 \cdot A_f^2 [W] \quad (8)$$

For useful floor area of the dwelling larger than 120 m^2 the value of Φ_{int} is simply equal to 450 W.

***$\Phi_{sol,t}$* – Directly Transmitted Solar Heat Gain**. Again based on ISO 52016–1:2017 [29], the directly transmitted solar gain is computed as per Equation (10).

$$\Phi_{sol,t} = \sum_{wi=1}^{n} \left[g_{wi,t}\left(I_{diff,eli,t} + I_{dir,eri,t} F_{sh,wi,t}\right) \cdot A_{wi}\left(1 - F_{fr,wi}\right)\right] [W] \quad (9)$$

where $g_{wi,t}$ (–) is the total solar energy transmittance of the window *wi*; $F_{sh,wi,t}$ (–) is the shading reduction factor accounting for the presence of external obstacles for window *wi*; $F_{fr,wi}$ (–) is the frame area fraction of window *wi*; and A_{wi} (m^2) is the surface area of window *wi*.

***$\varphi_{sky,eli,t}$* – Thermal Radiation to the Sky**. Accounts for the fraction of solar radiation that is dispersed to the sky and is computed by means of Equation 11, based on ISO 52016–1:2017 [29].

$$\varphi_{sky,eli,t} = F_{sky,eli} h_{re} \Delta\vartheta_{sky} \left[W \cdot m^{-2}\right] \quad (10)$$

where $F_{sky,eli}$ (–) is the view factor with respect to the sky, defined in the same ISO standard; h_{re} ($W \cdot m^{-2} \cdot K^{-1}$) is the external radiative surface heat transfer coefficient, chosen as in ISO 13789:2017 [28]; and $\Delta\vartheta_{sky}$ (K) is the average difference between the apparent sky temperature and the air temperature, whose indicative values are available in ISO 52016–1:2017 [29].

B.1.5 Dimensionless factors

f_{HC} – Convective Fraction of the HC Flux; f_{int} – Convective Fraction of the Internal Gains; f_{sol} – Convective Fraction of the Solar Radiation; a_{sol} – Solar Absorption Coefficient of External Surface (assumed for an intermediate colour; null for transparent elements); and F_{sh} – Shading Reduction Factor (representing the ratio between the actual direct irradiance on a building element and the direct solar irradiance on it in the ideal case of no obstacle presence in the surroundings) are all gathered from ISO 52016–1:2017 [29].

B.2 User behaviour and heating periods

As discussed in sub-section 2.2, the model follows a number of real-life relevant constraints. Table 5 reports the periods in which residential heating is allowed by the Italian legislation. Table 6 reports the three possible settings for sunlight hours (07:00–22:00), where the indoor comfort temperature set point is assumed to be 20 °C and the low set point 16 °C. Night-hour regulation is instead assumed to be identical among user types and fixed to the low set point. In particular, the following shares (among all Italian households) are identified for each setting: 25.3% for setting R1, 26.3% for setting R2 and 48.4% for setting R3.

B.5 Characteristics of Nearly Zero-Energy Buildings

The U-values obtained for NZEBs based on the method discussed in sub-section 2.3 are reported in Table 7 for the case of single-family buildings. Full numerical values for all archetypes are available at HeCo's open repository. Achieving such limit values requires significant enhancements of the insulation properties of existing buildings. Required transmittance reductions for vertical walls range from –82.4% to –16%, depending on the building geometry and climatic zone, whilst reductions in the transmittance of transparent surfaces (windows) range from –78.3% to –23.1%. The envelope renovation must be carried out through processes of thermal insulation coating; a proper insulating material needs to be added to roof, ground floor and walls, while windows needs to be substituted. For vertical walls, fiberglass is considered the preferable insulating material, and the thickness of the additional insulation is calculated for each case as reported in Table 8. Finally, it is worth noting that the U-value limits are intended by the Italian legislation as already comprehensive of all thermal bridges. For this reason, the overall thermal bridges transmittance (H_{tb}) is null for this category.

References

[1] Davis SJ, Lewis NS, Shaner M, Aggarwal S, Arent D, Azevedo IL, et al. Net-zero emissions energy systems. Science 2018;360. https://doi.org/10.1126/science.aas9793.
[2] Eurostat. Energy consumption in households - statistics explained. n.d,

https://ec.europa.eu/eurostat/statistics-explained/index.php?title=Energy_consumption_in_households#Energy_consumption_in_households_by_type_of_end-use. [Accessed 6 December 2019].
[3] Belussi L, Barozzi B, Bellazzi A, Danza L, Devitofrancesco A, Fanciulli C, et al. A review of performance of zero energy buildings and energy efficiency solutions. Journal of Building Engineering 2019;25:100772. https://doi.org/10.1016/j.jobe.2019.100772.
[4] European Commission. A Clean Planet for all. A European long-term strategic vision for a prosperous, modern, competitive and climate neutral economy 2018.
[5] Pfenninger S, Hawkes A, Keirstead J. Energy systems modeling for twenty-first century energy challenges. Renew Sustain Energy Rev 2014;33:74–86. https://doi.org/10.1016/j.rser.2014.02.003.
[6] Ruhnau O, Hirth L, Praktiknjo A. Time series of heat demand and heat pump efficiency for energy system modeling. Sci Data 2019;6:189. https://doi.org/10.1038/s41597-019-0199-y.
[7] Reiner Lemoine Institut. Demandlib documentation. n.d, https://demandlib.readthedocs.io/en/latest/index.html. [Accessed 4 March 2020].
[8] Pezzutto S, Zambotti S, Croce S, Zambelli P, Scaramuzzino C, Pascuas RP, et al. reportHotMaps D2.3 WP2 report – open data set for the EU28 [n.d].
[9] Georges E, Quoilin S, Mathieu S, Lemort V. Aggregation of flexible domestic heat pumps for the provision of reserve in power systems. Proceedings of ECOS 2017:12.
[10] Boßmann T, Staffell I. The shape of future electricity demand: exploring load curves in 2050s Germany and Britain. Energy 2015;90:1317–33. https://doi.org/10.1016/j.energy.2015.06.082.
[11] Brown T, Schlachtberger D, Kies A, Schramm S, Greiner M. Synergies of sector coupling and transmission reinforcement in a cost-optimised, highly renewable European energy system. Energy 2018;160:720–39. https://doi.org/10.1016/j.energy.2018.06.222.
[12] Connolly D, Drysdale D, Hansen K, Novosel T. reportSTRATEGO WP2 background report 2 - creating hourly profiles to model both demand and supply [n.d].
[13] Vivian J, Zarrella A, Emmi G, De Carli M. An evaluation of the suitability of lumped-capacitance models in calculating energy needs and thermal behaviour of buildings. Energy Build 2017;150:447–65. https://doi.org/10.1016/j.enbuild.2017.06.021.
[14] Clegg S, Mancarella P. Integrated electricity-heat-gas modelling and assessment, with applications to the Great Britain system. Part II: transmission network analysis and low carbon technology and resilience case studies. Energy 2019;184:191–203. https://doi.org/10.1016/j.energy.2018.02.078.
[15] Gendebien S, Georges E, Bertagnolio S, Lemort V. Methodology to characterize a residential building stock using a bottom-up approach: a case study applied to Belgium. International Journal of Sustainable Energy Planning and Management 2014;4:71–88. https://doi.org/10.5278/ijsepm.2014.4.7.
[16] Patteeuw D, Bruninx K, Arteconi A, Delarue E, D'haeseleer W, Helsen L. Integrated modeling of active demand response with electric heating systems coupled to thermal energy storage systems. Appl Energy 2015;151:306–19. https://doi.org/10.1016/j.apenergy.2015.04.014.
[17] Heinen S, Turner W, Cradden L, McDermott F, O'Malley M. Electrification of residential space heating considering coincidental weather events and building thermal inertia: a system-wide planning analysis. Energy 2017;127:136–54. https://doi.org/10.1016/j.energy.2017.03.102.
[18] Lombardi F, Rocco M, Locatelli S, Magni C, Colombo E, Belussi L, et al. Bottom-up lumped-parameters thermodynamic modelling of the Italian residential building stock: assessment of high-resolution heat demand profiles. IJES 2019;63:349–56. https://doi.org/10.18280/ti-ijes.632-434.
[19] ISO 52016-1. Energy performance of buildings - energy needs for heating and cooling, internal temperatures and sensible and latent heat loads Calculation procedures 2017. 2017. https://www.iso.org/standard/65696.html. [Accessed 11 August 2020].
[20] Lombardi F. SESAM-Polimi/HeCo. SESAM-Polimi; 2020.
[21] ISTAT. Istat - censimento popolazione. 2011.
[22] European Commission. EUR-Lex - 02010L0031-20181224 - EN - EUR-Lex. 2010. https://eur-lex.europa.eu/legal-content/EN/TXT/?uri=CELEX%3A02010L0031-20181224. [Accessed 5 May 2020].
[23] Ramallo-González AP, Eames ME, Coley DA. Lumped parameter models for building thermal modelling: an analytic approach to simplifying complex multi-layered constructions. Energy Build 2013;60:174–84. https://doi.org/10.1016/j.enbuild.2013.01.014.
[24] Corrado V, Ballarini I, Paduos S, Primo E, Madonna F. Application of dynamic numerical simulation to investigate the effects of occupant behaviour changes in retrofitted buildings. Proceedings of the 15th IBPSA Conference 2017:1862.–9.
[25] Italian Ministry of Economic Development. Decree of the Italian Ministry of Economic Development 26 June 2015 -Applicazione Delle Metodologie Di Calcolo Delle Prestazioni Energetiche e Definizione Delle Prescrizioni e Dei Requisiti Minimi Degli Edifici. 2015.
[26] Eurostat. Disaggregated final energy consumption in households. n.d, https://appsso.eurostat.ec.europa.eu/nui/show.do?dataset=nrg_d_hhq&lang=en. [Accessed 12 May 2020].
[27] UNI. UNI EN ISO 6946:2018. 2018. http://store.uni.com/catalogo/uni-en-iso-6946-2018?josso_back_to=http://store.uni.com/josso-security-check.php&josso_cmd=login_optional&josso_partnerapp_host=store.uni.com. [Accessed 15 October 2020].
[28] 14:00-17:00. ISO 13789:2017, Thermal performance of buildings — transmission and ventilation heat transfer coefficients — calculation method. ISO n.d. https://www.iso.org/cms/render/live/en/sites/isoorg/contents/data/standard/06/57/65713.html. [Accessed 15 October 2020].
[29] ISO. ISO 52016-1:2017, Energy performance of buildings - energy needs for heating and cooling, internal temperatures and sensible and latent heat loads Calculation procedures. 2017.
[30] Pfenninger S, Staffell I. Long-term patterns of European PV output using 30 years of validated hourly reanalysis and satellite data. Energy 2016;114:1251–65. https://doi.org/10.1016/j.energy.2016.08.060.
[31] UNI. UNI/TS 11300-1:2014, Prestazioni energetiche degli edifici - parte 1: determinazione del fabbisogno di energia termica dell'edificio per la climatizzazione estiva ed invernale. 2014. http://store.uni.com/catalogo/uni-ts-11300-1-2014. [Accessed 15 October 2020].

Nomenclature

a_{sol}: solar absorption coefficient of the external surfaces (–)
A_{eli}: surface area of the i-th building element (m^2)
A_{tot}: surface area of the total envelope (m^2)
A_f: useful floor area of the building (m^2)
A_{wi}: area of the window wi (m^2)
C_{int}: thermal capacity of internal air ($J \cdot K^{-1}$)
c_a: air specific heat ($kWh \cdot kg^{-1} \cdot K^{-1}$)
f_{HC}: convective fraction of the HC heat flux (–)
f_{int}: convective fraction of internal gains (–)
f_{sol}: convective fraction of solar gains (–)
F_{sh}: shading reduction factor (–)
$F_{sh,wi,t}$: shading reduction factor for window wi (–)
$F_{sky,eli}$: view factor to the sky (–)
$F_{fr,wi}$: frame area fraction of the window wi (–)
$g_{wi,t}$: total solar energy transmittance of the window wi (–)
$h_{ci,eli}$: internal surface convective heat transfer coefficient ($W \cdot m^{-2} \cdot K^{-1}$)
h_{eli}: building element heat transfer coefficient ($W \cdot m^{-2} \cdot K^{-1}$)◁
h_{re}: external radiative surface heat transfer coefficient ($W \cdot m^{-2} \cdot K^{-1}$)
h_{se}: external surface heat transfer coefficient ($W \cdot m^{-2} \cdot K^{-1}$)
H_{ve}: overall ventilation heat exchange coefficient ($W \cdot K^{-1}$)
H_{tb}: overall thermal bridges heat exchange coefficient ($W \cdot K^{-1}$)
$\kappa_{pli,eli}$: internal heat capacity of the i-th building element ($J \cdot m^{-2} \cdot K^{-1}$)
$I_{diff,eli,t}$: diffuse part of solar irradiation on the i-th element ($W \cdot m^{-2}$)
$I_{dir,eli,t}$: direct part of solar irradiation on the i-th element ($W \cdot m^{-2}$)
$l_{tb,k}$: length of linear thermal bridge k (m)
$q_{V,t}$: airflow rate ($m^3 \cdot s^{-1}$)
$T_{a,t}$: internal air temperature (K)
$T_{e,t}$: external (ambient) air temperature (K)
$T_{ext,eli,,t}$: i-th building element external surface temperature (K)
T_{int}: indoor ambient temperature (K)
$T_{int,eli,t}$: i-th building element internal surface temperature (K)
T_{set}: set point ambient temperature (K)
U: overall heat transfer coefficient ($W \cdot m^{-2} \cdot K^{-1}$)
Δt: time step (h)
$\Delta\vartheta_{sky}$: average diff. between apparent sky and air temperature (K)
$\phi_{sky,eli}$: radiative heat flux to the sky ($W \cdot m^{-2}$)
Φ_{HC}: total heating/cooling load (W)
Φ_{int}: total internal heat gain (W)
Φ_{sol}: directly transmitted heat gain (W)
ρ_a: air density ($kg \cdot m^{-3}$)
$\psi_{tb,k}$: linear thermal transmittance of a linear thermal bridge ($W \cdot m^{-1} \cdot K^{-1}$)

Acronyms

NZEB: Nearly Zero-Energy Building
P2H: Power-to-Heat
SLP: Standard Load Profile
RC: Resistance-Capacitance